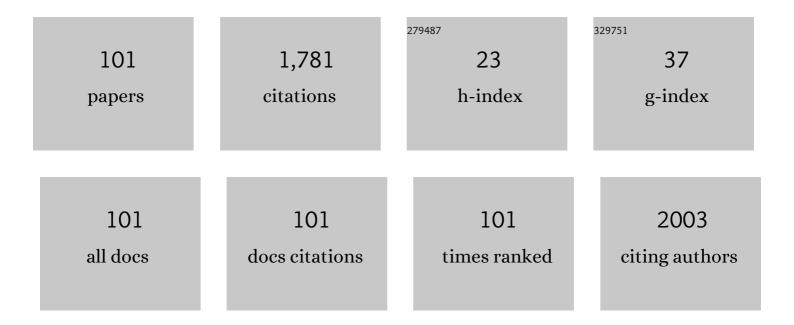
List of Publications by Year in descending order

Source: https://exaly.com/author-pdf/1440987/publications.pdf Version: 2024-02-01



FEDNANDO LAHOZ

#	Article	IF	CITATIONS
1	A Fluorescent Cage for Supramolecular Sensing of 3â€Nitrotyrosine in Human Blood Serum. Angewandte Chemie - International Edition, 2022, 61, .	7.2	16
2	FLTX2: A Novel Tamoxifen Derivative Endowed with Antiestrogenic, Fluorescent, and Photosensitizer Properties. International Journal of Molecular Sciences, 2021, 22, 5339.	1.8	4
3	Engineered Fluorescent Carbon Dots and G4-G6 PAMAM Dendrimer Nanohybrids for Bioimaging and Gene Delivery. Biomacromolecules, 2021, 22, 2436-2450.	2.6	25
4	Luminescent Nd ³⁺ â€Based Microresonators Working as Optical Vacuum Sensors. Advanced Optical Materials, 2020, 8, 2000678.	3.6	25
5	Er3+/Ho3+ codoped nanogarnet as an optical FIR based thermometer for a wide range of high and low temperatures. Journal of Alloys and Compounds, 2020, 847, 156541.	2.8	24
6	New insights into the blue intrinsic fluorescence of oxidized PAMAM dendrimers considering their use as bionanomaterials. Journal of Materials Chemistry B, 2020, 8, 10314-10326.	2.9	16
7	FRET mechanism between a fluorescent breast-cancer drug and photodynamic therapy sensitizers. Spectrochimica Acta - Part A: Molecular and Biomolecular Spectroscopy, 2020, 239, 118498.	2.0	2
8	Random lasing in brain tissues. Organic Electronics, 2019, 75, 105389.	1.4	30
9	Holmium doped fiber thermal sensing based on an optofluidic Fabry-Perot microresonator. Journal of Luminescence, 2019, 206, 492-497.	1.5	5
10	Luminescence whispering gallery modes in Ho3+ doped microresonator glasses for temperature sensing. Journal of Alloys and Compounds, 2019, 777, 198-203.	2.8	17
11	Opto-chemical and laser properties of FLTX1, a novel fluorescent tamoxifen derivative, and its potential applications in breast cancer photodynamic chemotherapy. Optical Materials, 2018, 84, 442-446.	1.7	3
12	Up-conversion processes in Ln(III)-doped luminescent materials for photovoltaics and photocatalysis. , 2018, , 291-333.		1
13	Multicolored Emission and Lasing in DCM-Adamantane Plasma Nanocomposite Optical Films. ACS Applied Materials & Interfaces, 2017, 9, 8948-8959.	4.0	12
14	A compact and portable optofluidic device for detection of liquid properties and label-free sensing. Journal Physics D: Applied Physics, 2017, 50, 215103.	1.3	7
15	Cadmium(ii) coordination polymers based on substituted malonic acid: synthesis, characterization and photoluminescence properties. Inorganic Chemistry Frontiers, 2017, 4, 1384-1392.	3.0	10
16	Enhanced green fluorescent protein in optofluidic Fabry-Perot microcavity to detect laser induced temperature changes in a bacterial culture. Applied Physics Letters, 2017, 111, .	1.5	4
17	Control of the luminescent properties of Eu2-xDyx(WO4)3 solid solutions for scintillator applications. Journal of Alloys and Compounds, 2017, 726, 796-802.	2.8	4
18	New fluorescent drug complex for opto-chemical therapy against breast cancer. , 2017, , .		0

#	Article	IF	CITATIONS
19	NIR upconversion emission of Tm 3+ doped glassceramics for solar cells applications. Journal of Luminescence, 2016, 179, 40-43.	1.5	12
20	Portable IR dye laser optofluidic microresonator as a temperature and chemical sensor. Optics Express, 2016, 24, 14383.	1.7	11
21	Luminescence and structural analysis of Ce ³⁺ and Er ³⁺ doped and Ce ³⁺ –Er ³⁺ codoped Ca ₃ Sc ₂ Si ₃ O ₁₂ garnets: influence of the doping concentration in the energy transfer processes. RSC Advances. 2016. 6. 15054-15061.	1.7	11
22	Analysis of the upconversion process in Tm3+ doped glasses for enhancement of the photocurrent in silicon solar cells. Solar Energy Materials and Solar Cells, 2016, 144, 29-32.	3.0	24
23	From Broad-Spectrum Biocides to Quorum Sensing Disruptors and Mussel Repellents: Antifouling Profile of Alkyl Triphenylphosphonium Salts. PLoS ONE, 2015, 10, e0123652.	1.1	54
24	Nano-to millisecond lifetime luminescence properties in Ln2(WO4)3 (LnÂ=ÂLa, Ho, Tm and Eu) microcrystalline powders with different crystal structures. Journal of Alloys and Compounds, 2015, 649, 1253-1259.	2.8	15
25	Synthesis, characterization and solid-state photoluminescence studies of six alkoxy phenylene ethynylene dinuclear palladium(<scp>ii</scp>) rods. Dalton Transactions, 2015, 44, 4003-4015.	1.6	5
26	Random laser in biological tissues impregnated with a fluorescent anticancer drug. Laser Physics Letters, 2015, 12, 045805.	0.6	57
27	Slow magnetic relaxation and photoluminescent properties of a highly coordinated erbium(iii) complex with dibenzoylmethane and 2,2′-bipyridine. New Journal of Chemistry, 2015, 39, 1703-1713.	1.4	17
28	Synthesis, structural modelling and luminescence of a novel erbium(III) complex with 2,4-nonanedione and 2,2′-bipyridine ligands for chitosan matrices doping. Optical Materials, 2015, 41, 139-142.	1.7	8
29	An erbium(III)-based NIR emitter with a highly conjugated β-diketonate for blue-region sensitization. Journal of Alloys and Compounds, 2015, 619, 553-559.	2.8	21
30	Whispering gallery mode laser enhanced by amplified spontaneous emission coupling in semiconducting polymer solutions. Laser Physics Letters, 2014, 11, 046001.	0.6	6
31	Highly fluorinated erbium(III) complexes for emission in the C-band. Journal of Photochemistry and Photobiology A: Chemistry, 2014, 292, 16-25.	2.0	17
32	Thermally induced whispering gallery mode laser in MEH-PPV solutions. Organic Electronics, 2014, 15, 1923-1927.	1.4	1
33	High efficiency amplified spontaneous emission from a fluorescent anticancer drug–dye complex. Organic Electronics, 2013, 14, 1225-1230.	1.4	14
34	Structure and NIR-luminescence of ytterbium(iii) beta-diketonate complexes with 5-nitro-1,10-phenanthroline ancillary ligand: assessment of chain length and fluorination impact. Dalton Transactions, 2013, 42, 13516.	1.6	38
35	Mechanism of millisecond lifetime luminescence of Li nanoclusters dispersed in ZnO:Li nanocrystals. Optical Materials, 2013, 35, 638-643.	1.7	1

36 Optical gain and laser emission in fluorescent drug nanocomposites. , 2013, , .

0

#	Article	IF	CITATIONS
37	Novel erbium(iii) complexes with 2,6-dimethyl-3,5-heptanedione and different N,N-donor ligands for ormosil and PMMA matrices doping. Journal of Materials Chemistry C, 2013, 1, 5701.	2.7	35
38	Unique SERM-like properties of the novel fluorescent tamoxifen derivative FLTX1. European Journal of Pharmaceutics and Biopharmaceutics, 2013, 85, 898-910.	2.0	19
39	Whispering gallery mode laser based on antitumor drug–dye complex gain medium. Optics Letters, 2012, 37, 4756.	1.7	18
40	Synthesis, structural analysis, and thermal and spectroscopic studies of methylmalonate-containing zinc(II) complexes. Comptes Rendus Chimie, 2012, 15, 911-923.	0.2	6
41	Upconversion mechanisms in rare-earth doped glasses to improve the efficiency of silicon solar cells. Solar Energy Materials and Solar Cells, 2011, 95, 1671-1677.	3.0	99
42	Optical gain by upconversion in Tm–Yb oxyfluoride glass ceramic. Applied Physics B: Lasers and Optics, 2011, 104, 237-240.	1.1	1
43	Complete energy transfer due to rare-earth phase segregation in optical fiber preform glasses. Journal of Applied Physics, 2011, 110, 083121.	1.1	4
44	Stimulated emission in the red, green, and blue in a nanostructured glass ceramics. Journal of Applied Physics, 2011, 109, 043102-043102-6.	1.1	9
45	Structural changes induced on strontium barium niobate glass byÂfemtosecond laser irradiation. Applied Physics A: Materials Science and Processing, 2010, 98, 879-884.	1.1	4
46	Optical amplification by upconversion in Tm–Yb fluoroindate glass. Optical Materials, 2010, 32, 1349-1351.	1.7	9
47	Optical gain in Er3+-doped transparent LuVO4 crystal at 850nm. Optical Materials, 2010, 32, 475-478.	1.7	8
48	Optical amplification in Er3+-doped transparent Ba2NaNb5O15 single crystal at 850 nm. Journal of Applied Physics, 2009, 106, 113108.	1.1	8
49	Polymeric waveguides using oxidized porous silicon cladding for optical amplification. Optical Materials, 2009, 31, 1488-1491.	1.7	10
50	Optical amplification in Er3+-doped fluoroindate glass at 840nm and 1550nm. Optical Materials, 2009, 31, 1370-1372.	1.7	6
51	Reduction of the amplified spontaneous emission threshold in semiconducting polymer waveguides on porous silica. Optics Express, 2009, 17, 16766.	1.7	24
52	Upconversion emission in Er3+-doped lead niobium germanate thin-film glasses produced by pulsed laser deposition. Applied Physics A: Materials Science and Processing, 2008, 93, 621-625.	1.1	6
53	Localized desvitrifiation in Er3+-doped strontium barium niobate glass by laser irradiation. Applied Physics A: Materials Science and Processing, 2008, 93, 977-981.	1.1	6
54	Local crystallization in an oxyfluoride glass doped with Er3+ ions using a continuous argon laser. Applied Physics A: Materials Science and Processing, 2008, 93, 983-986.	1.1	4

#	Article	IF	CITATIONS
55	Desvitrification on an oxyfluoride glass doped with Tm3+ and Yb3+ ions under Ar laser irradiation. Journal of Luminescence, 2008, 128, 905-907.	1.5	9
56	Increase of the blue upconversion emission in YAG:Tm3+ nanopowders by codoping with Yb3+ ions. Journal of Luminescence, 2008, 128, 924-926.	1.5	14
57	Optical properties of Er3+-doped strontium barium niobate nanocrystals obtained by thermal treatment in glass. Journal of Luminescence, 2008, 128, 908-910.	1.5	28
58	Optical gain in conjugated polymer hybrid structures based on porous silicon waveguides. Chemical Physics Letters, 2008, 463, 387-390.	1.2	9
59	Efficient blue upconversion emission due to confined radiative energy transfer in Tm3+–Nd3+ co-doped Ta2O5 waveguides under infrared-laser excitation. Optics Communications, 2008, 281, 3691-3694.	1.0	18
60	Effect of pressure on the luminescence properties of Nd3+ doped SrWO4 laser crystal. Journal of Alloys and Compounds, 2008, 451, 212-214.	2.8	21
61	Ho^3+-doped nanophase glass ceramics for efficiency enhancement in silicon solar cells. Optics Letters, 2008, 33, 2982.	1.7	50
62	Supramolecular Networks in Copper(II) Malonate Complexes. Crystal Growth and Design, 2008, 8, 3219-3232.	1.4	48
63	Optical amplification in Ho3+-doped transparent oxyfluoride glass ceramics at 750nm. Applied Physics Letters, 2007, 90, 201117.	1.5	26
64	Optical gain in dye-doped polymer waveguides using oxidized porous silicon cladding. , 2007, , .		2
65	Temperature dependence of Nd3+→Yb3+ energy transfer processes in co-doped oxyfluoride glass ceramics. Journal of Non-Crystalline Solids, 2007, 353, 1951-1955.	1.5	23
66	Stimulated emission and light amplification in Ho3+doped oxyfluoride glasses and glass-ceramics. , 2007, , .		0
67	Energy transfer in Pr3+–Yb3+ codoped oxyfluoride glass ceramics. Optical Materials, 2007, 29, 1231-1235.	1.7	8
68	Optical gain in oxidized porous silicon waveguides impregnated with a laser dye. Physica Status Solidi C: Current Topics in Solid State Physics, 2007, 4, 2145-2149.	0.8	0
69	Dopant partitioning influence on the near-infrared emissions of Tm3+ in oxyfluoride glass ceramics. Journal of Applied Physics, 2006, 99, 053103.	1.1	23
70	High-pressure luminescence in Nd3+-doped MgO:LiNbO3. High Pressure Research, 2006, 26, 341-344.	0.4	11
71	Analysis of the Eu3+emission in a SrWO4laser matrix under pressure. High Pressure Research, 2006, 26, 355-359.	0.4	13
72	Room temperature infrared-laser-induced upconversion in Nd3+ doped Ta2O5 waveguides. Chemical Physics Letters, 2006, 421, 198-204.	1.2	7

#	Article	IF	CITATIONS
73	Upconversion rate in Nd-doped Ta2O5 waveguides and influence on the cw laser performance. Chemical Physics Letters, 2006, 426, 135-140.	1.2	5
74	Optical gain in dye-impregnated oxidized porous silicon waveguides. Applied Physics Letters, 2006, 89, 011107.	1.5	24
75	Infrared-to-visible photon avalanche upconversion dynamics in Ho3+-doped fluorozirconate glasses at room temperature. Optical Materials, 2005, 27, 1754-1761.	1.7	40
76	Rare earths in nanocrystalline glass–ceramics. Optical Materials, 2005, 27, 1762-1770.	1.7	62
77	Porous silicon-based notch filters and waveguides. , 2005, , .		3
78	Neodymium-doped tantalum pentoxide waveguide lasers. IEEE Journal of Quantum Electronics, 2005, 41, 1565-1573.	1.0	33
79	Ultraviolet and white photon avalanche upconversion in Ho3+-doped nanophase glass ceramics. Applied Physics Letters, 2005, 86, 051106.	1.5	70
80	Temperature dependence of Nd3+↔Yb3+ energy transfer in the YAl3(BO3)4 nonlinear laser crystal. Journal of Applied Physics, 2005, 97, 093510.	1.1	30
81	Theoretical analysis of the photon avalanche dynamics in Ho3+-Yb3+ codoped systems under near-infrared excitation. Physical Review B, 2005, 71, .	1.1	17
82	Dopant distribution in a Tm3+–Yb3+ codoped silica based glass ceramic: An infrared-laser induced upconversion study. Journal of Chemical Physics, 2004, 120, 6180-6190.	1.2	157
83	Room temperature photon avalanche up-conversion in Ho3+ doped fluoroindate glasses under excitation at 747 nm. Optical Materials, 2004, 25, 209-213.	1.7	18
84	Optical properties of Eu3+ ions in malonate crystals to monitor a structural phase transition. Optical Materials, 2004, 25, 223-229.	1.7	7
85	Infrared-laser induced photon avalanche upconversion in Ho3+–Yb3+ codoped fluoroindate glasses. Journal of Applied Physics, 2004, 95, 2957-2962.	1.1	50
86	Optical intensities of Pr3+ ions in transparent oxyfluoride glass and glass–ceramic. Applications of the standard and modified Judd–Ofelt theories. Journal of Alloys and Compounds, 2004, 380, 167-172.	2.8	48
87	Optical properties and upconversion in Yb3+—Tm3+co-doped oxyfluoride glasses and glass ceramics. Molecular Physics, 2003, 101, 1057-1065.	0.8	21
88	Room temperature photon avalanche upconversion in Ho3+doped fluoroindate glasses under excitation at 749 nm. , 2003, 4829, 141.		0
89	Optical properties of Eu3+in malonate crystals to monitor a structural phase transition. , 2003, , .		0
90	1.3-/spl mu/m emission of Nd:LaF/sub 3/ thin films grown by molecular beam epitaxy. IEEE Journal of Quantum Electronics, 2000, 36, 243-247.	1.0	14

#	Article	IF	CITATIONS
91	Infrared-laser-induced upconversion fromNd3+:LaF3heteroepitaxial layers onCaF2(111)substrates by molecular beam epitaxy. Physical Review B, 2000, 62, 4446-4454.	1.1	26
92	Hetero- and homoepitaxial Nd3+-doped LaF3 thin films grown by molecular beam epitaxy: A spectroscopic study. Journal of Applied Physics, 1999, 86, 3699-3704.	1.1	5
93	CaF2:Yb3++Pr3+ codoped waveguides grown by molecular beam epitaxy for 1.3 μm applications. Applied Physics Letters, 1999, 74, 1060-1062.	1.5	8
94	Optical properties of Mn2+ ions in solid solutions of fluorite-type crystals. Journal of Luminescence, 1999, 81, 53-60.	1.5	12
95	Local disorder and structural phase transition in Rb1 â^ xCsxCaF3:Ni+ crystals studied by EPR. Journal of Physics and Chemistry of Solids, 1998, 59, 981-988.	1.9	2
96	Cubic-to-tetragonal structural phase transition inRb1â^'xCsxCaF3solid solutions: Thermal expansion and EPR studies. Physical Review B, 1997, 55, 8148-8154.	1.1	3
97	Influence of the host lattice on the photoluminescence of Ni2+ ions in Rb1â^'xCsxCaF3 and RbCa1â^'xCdxF3 crystals. Journal of Applied Physics, 1997, 82, 5121-5125.	1.1	1
98	THE TETRAGONAL TO ORTHORHOMBIC STRUCTURAL PHASE TRANSITION IN RbCaF 3 SINGLE CRYSTALS: INFLUENCE ON THE LOCAL ENVIRONMENT OF DIFFERENT NICKEL PROBES. Journal of Physics and Chemistry of Solids, 1997, 58, 881-892.	1.9	12
99	Spectroscopic properties of Mn ²⁺ ions in mixed fluoroperovskites. Radiation Effects and Defects in Solids, 1995, 135, 163-167.	0.4	2
100	Mn2+as a probe in RbCaF3: local order parameter of the structural phase transition measured by ENDOR. Journal of Physics Condensed Matter, 1995, 7, 8637-8645.	0.7	6
101	A Fluorescent Cage for Supramolecular Sensing of 3â€Nitrotyrosine in Human Blood Serum. Angewandte Chemie, 0, , .	1.6	2